"Axial-Bonding"-Type Hybrid Porphyrin Arrays: Synthesis, Spectroscopy, Electrochemistry, and Singlet State Properties

L. Giribabu, T. Anita Rao, and Bhaskar G. Maiya*,†

School of Chemistry, University of Hyderabad, Hyderabad, 500 046, India

Received March 23, 1999

A series of phosphorus(V), germanium(IV), and tin(IV) porphyrin-based, "axial-bonding"-type hybrid trimers have been readily constructed by employing a new "building-block" approach. The approach is modular in nature, and it involves simple "inorganic" reactions such as axial bond formation of main group element containing porphyrins and insertion of metal/"metalloid" ions into the porphyrin cavity. The architecture of these arrays is such that, while a phosphorus(V), germanium(IV), or tin(IV) complex of *meso*-5,10,15,20-(tetratolyl)porphyrin forms the basal scaffolding unit, the free-base, vanadyl, cobalt(II), nickel(II), copper(II), or zinc(II) porphyrins occupy the two axial sites via an aryloxy bridge. Synthesis of an "all-phosphorus" array containing three phosphorus(V) subunits has also been accomplished. Each new porphyrin array investigated in this study has been fully characterized by various physical methods that include mass (FAB), UV−visible, infrared, fluorescence, electron spin resonance (ESR), and ^{1}H and ^{31}P nuclear magnetic resonance (NMR; 1D and 2D) spectroscopies and cyclic voltammetry. The UV−visible and ESR spectral parameters and also the redox potential data suggest that there exists no interaction between the π-planes of the constituent monomeric porphyrins in these arrays. Detailed ^{1}H NMR investigations carried out with the trimers containing diamagnetic porphyrins reveal characteristic shielding/deshielding effects for the various protons on the axial porphyrin subunits. The ground state data, as probed by the spectroscopic and electrochemical techniques, collectively indicate that there exists a symmetric but nonparallel disposition of the two axial porphyrins with respect to plane of the central porphyrin. Singlet state activity of the photoactive trimers has been probed by the steady state fluorescence method with selective excitation into the bands corresponding to the two constituent monomeric species. Analysis of the fluorescence emission and excitation spectral data suggests the occurrence of electronic energy transfer as well as photoinduced electron transfer reactions in trimers endowed with free-base or zinc(II) porphyrin axial subunits. Efficiencies of the excited state processes of these trimeric arrays are shown to be dependent on the type of metal/metalloid ions present in the porphyrin crevice.

Introduction

Photochemically active supramolecular arrays composed of porphyrin or other structurally related macrocyclic systems are currently being investigated in connection with their ability to transport charge, ions, or energy.[1−23] A great variety of homologous porphyrin arrays has been reported so far but, relatively less attention seems to have been paid toward the construction of functionally active, hybrid-type systems with fine-tunable photo- and electrochemical properties. Moreover, the majority of the hitherto reported porphyrin arrays (hybrid or otherwise) have been obtained via multistep and often cumbersome organic reaction sequences carried out at the porphyrin peripheral position(s). On the other hand, utilization of "inorganic" reactions, which can be readily conducted either at the porphyrin central cavity (e.g., metal/nonmetal ion insertion) or on the resident metal/metalloid ion therein (e.g., metal−metal interaction, metal−ligand coordination, covalent bond formation, etc.), appears to be an attractive and a viable

† E-mail: bgmsc@uohyd.ernet.in.

(1) van Nostrum, C. F.; Nolte, R. J. M. *J. Chem. Soc., Chem. Commun.* **1996**, 2385.
(2) Gust, D.; Moore, T. A.; Moore, A. L. *Acc. Chem. Res*. **1993**, *26*, 198.
(3) Anderson, S.; Anderson, H. L.; Sanders, J. K. M. *Acc. Chem. Res.* **1993**, *26*, 469.
(4) Wasielewski, M. R. *Chem. Rev*. **1992**, *92*, 435.
(5) Chichak, K.; Branda, N. R. *J. Chem. Soc. Chem. Commun*. **1999**, 523.
(6) Beavington, R.; Burn, P. L. *J. Chem. Soc., Perkin Trans. 1* **1999**, 583.
(7) Ogawa, T.; Nishimoto, Y.; Yoshida, N.; Ono, N.; Osuka, A. *Angew. Chem., Int. Ed.* **1999**, *38*, 176.
(8) Mak, C. C.; Bampos, N.; Sanders, J. K. M. *Angew. Chem., Int. Ed.* **1998**, *37*, 3020.
(9) Nakano, A.; Osuka, A.; Yamazaki, I.; Yamazaki, T.; Nishimura, Y. *Angew. Chem., Int. Ed.* **1998**, *37*, 3023.
(10) Strachan, J.; Gentemann, S.; Seth, J.; Kalasbeck, W. A.; Lindsey, J. S.; Holten, D.; Bocian, D. F. *Inorg. Chem*. **1998**, *37*, 1191.
(11) Marty, M.; Clyde-Watson, Z.; Twyman, L. J.; Nakash, M.; Sanders, J. K. M. *Chem. Commun. (Cambridge)* **1998**, 2265.
(12) Vicente, M. G. H.; Cancilla, M. T.; Lebrilla, C. B.; Smith, K. M. *Chem. Commun*. *(Cambridge)* **1998**, 2355.
(13) Osuka, A.; Shimidzu, H. *Angew. Chem., Int. Ed. Engl*. **1997**, *36*, 135.
(14) Ema, T.; Misawa, S.; Nemugaki, S.; Utaka, M. *Chem. Lett*. **1997**, 487.
(15) Officer, D. L.; Burrel, A. K.; Reid, D. C. W. *Chem. Commun*. *(Cambridge)* **1996**, 1657.
(16) Susumu, K.; Shimidzu, T.; Tanaka, K.; Segawa, H. *Tetrahedron Lett*. **1996**, *37*, 8399.
(17) Reimers, J. R.; Lu, T. X.; Crossley, M. J.; Hush, N. S. *Chem. Phys. Lett*. **1996**, *256*, 353.
(18) Chernook, A. V.; Rempel, U.; Borczyskowski, C. V.; Shulga, A. M.; Senkevich, E. *Chem. Phys. Lett*. **1996**, *254*, 229.
(19) Chernook, A. V.; Rempel, U.; Borczyskowski, C. V.; Shulga, A. M.; Senkevich, E. *Chem. Phys. Lett*. **1996**, *254*, 229.
(20) Collman, J. P.; Ennis, M. S.; Offord, D. A.; Chng, L. L.; Griffin, J. H. *Inorg. Chem*. **1996**, *35*, 1751.
(21) Anderson, H. L. *Inorg. Chem*. **1994**, *33*, 972.
(22) Chambron, J.-C.; Harriman, A.; Heitz, V.; Sauvage, J.-P. *J. Am. Chem. Soc*. **1993**, *115*, 7419.
(23) Sessler, J. L.; Capuano, V. L.; Harriman, A. *J. Am. Chem. Soc*. **1993**, *115*, 4577 and references therein.

10.1021/ic990326c CCC: $18.00
Published on Web 10/13/1999

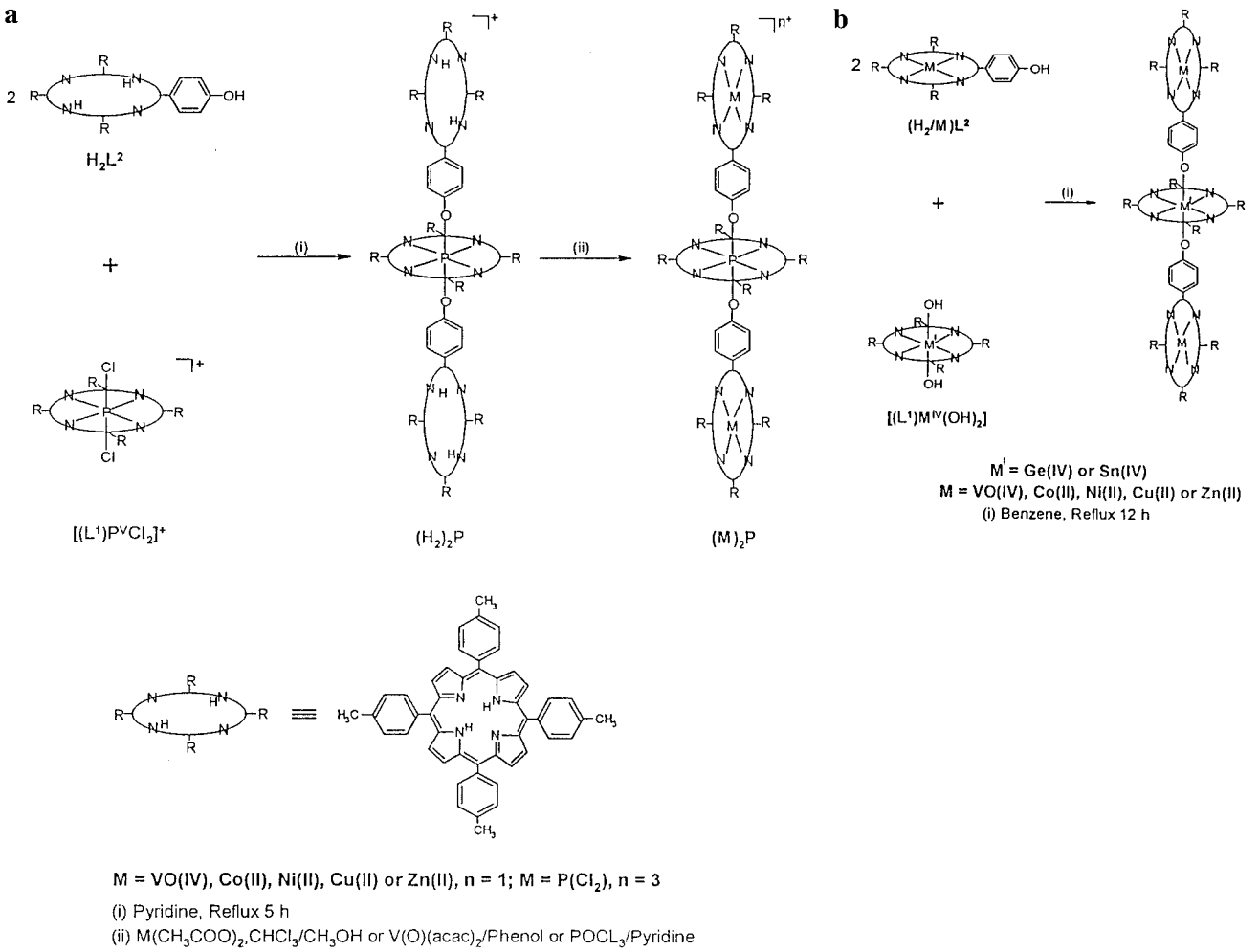

Figure 1. Schemes leading to the synthesis of various "axial-bonding"-type hybrid trimers investigated in this study.

alternative approach for the facile construction of hybrid-type multiporphyrin arrays.[24−42]

During the course of our recent investigations on the donor−acceptor type, hexacoordinated, bis(aryloxo)phosphorus(V) (P^V) porphyrins which also include a few trimeric systems,[43,44] we realized that the inherent simplicity and the flexibility of our new, "axial-bonding" approach can be conveniently employed for the design and synthesis of more elaborate, hybrid-type, porphyrin arrays having diverse structures and functions. For example, it should be possible to utilize different, photochemically active, main group element containing porphyrins[45] as the basal scaffolding units and free-base porphyrins, metalloporphyrins, or metalloid porphyrins as the axial donor/acceptor subunits for the fabrication of arrays with varying spectral, redox, and photophysical properties. This is indeed the case as will be demonstrated in this paper, which reports on the design, synthesis, and modulation of the redox and photochemical functions of a series of P^V, germanium(IV) (Ge^{IV}), and tin(IV) (Sn^{IV}) porphyrin-based, "axial-bonding"-type hybrid trimers, Figure 1.

Experimental Section

A. Materials. 1. General. The chemicals and solvents utilized in this study were purchased from either Aldrich Chemical Co. (U.S.A.)

(24) Sharma, C. V. K.; Broker, G. A.; Huddleston, J. G.; Baldwin, J. W.; Metzger, R. M.; Rodgers, R. D. *J. Am. Chem. Soc.* **1999**, *121*, 1137.
(25) Kumar, R. K.; Goldber, I. *Angew. Chem., Int. Ed.* **1998**, *37*, 3027.
(26) Drain, C. M.; Nifiatis, F.; Vasenko, A.; Batteas, J. D. *Angew. Chem., Int. Ed.* **1998**, *37*, 2344.
(27) Gerasimchuk, N. N.; Mokhir, A. A.; Rodgers, K. R. *Inorg. Chem.* **1998**, *37*, 5641.
(28) Funatsu, K.; Imamura, T.; Ichimura, A.; Sasaki, Y. *Inorg. Chem.* **1998**, *37*, 4986.
(29) Funatsu, K.; Imamura, T.; Ichimura, A.; Sasaki, Y. *Inorg. Chem.* **1998**, *37*, 1798.
(30) Strachan, J.; Gentemann, S.; Seth, J.; Kalasbeck, W. A.; Lindsey, J. S.; Holten, D.; Bocian, D. F. *Inorg. Chem.* **1998**, *37*, 1191.
(31) Kumar, R. K.; Balasubramanian, S.; Goldberg, I. *Inorg. Chem.* **1998**, *37*, 541.
(32) Alessio, E.; Macchi, M.; Heath, S. L.; Marzilli, L. G. *Inorg. Chem.* **1997**, *36*, 5614.
(33) Solne, R. V.; Hupp, J. T. *Inorg. Chem.* **1997**, *36*, 5422.
(34) Kariya, N.; Imamura, T.; Sasaki, Y. *Inorg. Chem.* **1997**, *36*, 833.
(35) Endo, A.; Tagami, U.; Wada, Y.; Saito, M.; Shimizu, K.; Sato, G. P. *Chem. Lett.* **1996**, 213.
(36) Alessio, E.; Macchi, M.; Heath, S.; Marzilli, L. G. *Chem. Commun. (Cambridge)* **1996**, 1411.
(37) Ruhlmann, L.; Giraudeau, A. *Chem. Commun. (Cambridge)* **1996**, 2007.
(38) Wojaczynski, J.; Latos-Grazumslo, L. *Inorg. Chem.* **1996**, *35*, 4812.
(39) Yuan, H.; Thomas, L.; Woo, L. K. *Inorg. Chem.* **1996**, *35*, 2808.
(40) Susumu, K.; Segawa, H.; Shimidzu, T. *Chem. Lett.* **1995**, 929.
(41) Susumu, K.; Kunimoto, K.; Segawa, H.; Shimidzu, T. *J. Phys. Chem.* **1995**, *99*, 29.
(42) Segawa, H.; Kunimoto, K.; Susumu, K.; Taniguchi, M.; Shimidzu, T. *J. Am. Chem. Soc.* **1994**, *116*, 11193.
(43) Rao, T. A.; Maiya, B. G. *Inorg. Chem.* **1996**, *35*, 4829.
(44) Rao, T. A.; Maiya, B. G. *J. Chem. Soc., Chem. Commun.* **1995**, 939.
(45) The majority of main group element containing porphyrins have been reported to show strong luminescence (Sayer, P.; Gouterman, M.; Connell, C. R. *Acc. Chem. Res.* **1982**, *15*, 73) as against the transition metal porphyrins, most of which, being paramagnetic, are relatively less luminescent.

or B.D.H. (Mumbai, India). The solvents utilized for spectroscopic and electrochemical experiments were further purified using standard procedures.[46]

2. Synthesis. The *meso*-5,10,15,20-(tetratolyl)porphyrin (H_2L^1) and its metalloid/metal complexes $[(L^1)P^{V}Cl_2]^+$, $[(L^1)P^{V}(OH)_2]^+$, $[(L^1)Ge^{IV}(OH)_2]$, $[(L^1)Sn^{IV}(OH)_2]$, $[(L^1)V^{IV}(O)]$, $[(L^1)Co^{II}]$, $[(L^1)Ni^{II}]$, $[(L^1)Cu^{II}]$, and $[(L^1)Zn^{II}]$ were synthesized and purified according to the reported procedures.[47−50] The *meso*-5-(4-hydroxyphenyl)-10,15,20-(tritolyl)porphyrin (H_2L^2)[51] and its derivatives $[(L^2)V^{IV}(O)]$, $[(L^2)Co^{II}]$, $[(L^2)Ni^{II}]$, $[(L^2)Cu^{II}]$, and $[(L^2)Zn^{II}]$ were also synthesized by adapting similar procedures. Synthesis of the trimeric arrays is detailed below (see Figure 1, schemes a and b).

$(H_2)_2$P. $[(L^1)P^{V}Cl_2]^+$ (100 mg, 0.13 mmol) was dissolved in 25 mL of dry pyridine, and to this solution was added 400 mg (0.59 mmol) of H_2L^2. The mixture was refluxed under a nitrogen atmosphere for 5 h. The solvent was evaporated, and the resulting brown residue, dissolved in 5 mL of $CHCl_3$, was loaded onto a silica gel column. The desired product, as its hydroxide salt, was eluted with $CHCl_3-CH_3OH$ (9:1, v/v), after which it was recrystallized using a $CHCl_3$−hexane mixture. Yield: 50%. MS: (*m*/*z*) (M = $C_{142}H_{106}N_{12}O_2P$) 2059, $[M + OH]^+$; 2042, $[M]^+$; 1370, $[M - C_{47}H_{35}N_4O]^+$; 699, $[M - 2(C_{47}H_{35}N_4O)]^+$; 673, $[C_{47}H_{36}N_4O]^+$. UV−visible (CH_2Cl_2): λ_{nm} (log ϵ) 420 (6.02), 441 (5.40), 517 (4.49), 555 (4.40), 592 (4.16), 648 (4.00).

$(VO)_2$P, $(Co)_2$P, $(Ni)_2$P, $(Cu)_2$P, and $(Zn)_2$P. Method 1. In the first method, these trimers were prepared in a manner analogous to that described above for the synthesis of $(H_2)_2$P, but by replacing H_2L^2 with the corresponding metalloporphyrins. In each case, 50 mg (0.065 mmol) of $[(L^1)P^{V}Cl_2]^+$ was refluxed with excess (0.3−0.4 mmol) $[(L^2)M]$ (M = $V^{IV}(O)$, Co^{II}, Ni^{II}, Cu^{II} or Zn^{II}) in 15 mL of dry pyridine under a nitrogen atmosphere for 5−6 h. Pyridine was evaporated, and the solid obtained was loaded onto a silica gel column. The desired product was eluted with $CHCl_3-CH_3OH$ (9:1, v/v), after which it was recrystallized using a $CHCl_3$−hexane mixture. Yields ranged typically between 50% and 60%.

Method 2. This method involves metalation of the two axial free-base porphyrins of $(H_2)_2$P by the standard methods.[47] Refluxing 10 mg (0.0046 mmol) of $(H_2)_2$P dissolved in 20 mL of $CHCl_3$ with 15 mg of the corresponding metal acetates dissolved in 5 mL of CH_3OH for 0.5 h gave $(Co)_2$P, $(Ni)_2$P, $(Cu)_2$P, and $(Zn)_2$P. Ca. 0.2 mL of acetic acid was also added to the reaction mixture in the case of metalation with copper(II). Evaporation of the solvents and the subsequent purification of the solids by column chromatography (silica gel; $CHCl_3-CH_3OH$, 9:1, v/v) and recrystallization ($CHCl_3$−hexane) gave the desired product in >90% yields in each case. Insertion of $V^{IV}(O)$ into the axial porphyrins was achieved by mixing 15 mg (0.007 mmol) of $(H_2)_2$P and 15 mg (0.09 mmol) of vanadyl acetylacetonate in 5 mL of phenol and refluxing the resulting solution for 0.5 h. Phenol was removed under reduced pressure, and the crude product was purified as described above for the other metallo/"metalloid" porphyrins (yield: 70%). UV−visible (CH_2Cl_2): λ_{nm} (log ϵ), $(VO)_2$P, 426 (5.75), 443 (5.47), 552 (4.54), 609 (4.06); Co_2P, 414 (5.34), 436 (5.52), 529 (4.37), 562 (4.40), 607 (4.05); Ni_2P, 416 (5.63), 438 (5.32), 528 (4.50), 561 (4.29), 609 (3.94); Cu_2P, 416 (5.84), 440 (5.28), 540 (4.58), 567 (4.27), 608 (3.92); Zn_2P, 421 (5.76), 445 (5.13), 551 (4.62), 587 (4.20), 611 (3.99).

P_3. Phosphorus oxychloride ($POCl_3$) (0.16 g, ∼1 mmol) was added to $(H_2)_2$P (100 mg, 0.046 mmol) dissolved in dry pyridine (30 mL) in an atmosphere of nitrogen. The mixture was refluxed for 24 h under nitrogen. The solvent pyridine and excess $POCl_3$ were removed under reduced pressure. The solid obtained was chromatographed on a silica gel column. Elution with $CHCl_3-CH_3OH$ (9:1, v/v) gave a green solid, which was further purified by recrystallization from C_6H_6−octane to give P_3 in ≅70% yield. UV−visible (CH_2Cl_2): λ_{nm} (log ϵ) 445 (5.85), 571 (4.56), 618 (4.42).

$(H_2)_2$Ge. $[(L^1)Ge^{IV}(OH)_2]$ (100 mg, 0.13 mmol) was dissolved in 30 mL of dry C_6H_6. To this was added 192 mg (0.29 mmol) of H_2L^2, and the resulting solution was refluxed under a nitrogen atmosphere for 12 h. The solvent was evaporated, and the solid obtained was loaded onto a neutral alumina column. The desired product was eluted with $CHCl_3$, after which it was recrystallized using a CH_2Cl_2−hexane mixture. Yield: 60%. MS: *m*/*z* $(H_2)_2Ge$ ($C_{142}H_{106}N_{12}O_2Ge$) 2085, $[M]^+$; 1412, $[M - (C_{47}H_{35}N_4O) + H]^+$; 741, $[M - 2(C_{47}H_{35}N_4O)]^+$; 673, $[C_{47}H_{36}N_4O]^+$. UV−visible (CH_2Cl_2): λ_{nm} (log ϵ) 420 (5.67), 518 (4.43), 559 (4.47), 602 (4.28), 651 (4.14).

$(VO)_2$Ge, $(Co)_2$Ge, $(Ni)_2$Ge, $(Cu)_2$Ge, and $(Zn)_2$Ge. These trimers were prepared in a manner analogous to that described above for the synthesis of $(H_2)_2$Ge, but by replacing H_2L^2 with the corresponding metalloporphyrins. In each case, 50 mg (0.065 mmol) of $[(L^1)Ge^{IV}(OH)_2]$ was refluxed with an excess (0.3−0.4 mmol) of $[(L^2)M]$ (M = $V^{IV}(O)$, Co^{II}, Ni^{II}, Cu^{II}, and Zn^{II}) in dry C_6H_6 under a nitrogen atmosphere for 12−16 h. The solvent was evaporated, and the resulting solids were purified as described above for $(H_2)_2$Ge. Yields ranged typically between 50% and 60%. UV−visible (CH_2Cl_2): λ_{nm} (log ϵ), $(VO)_2$Ge, 425 (5.61), 517 (3.79), 551 (4.56), 593 (4.03); Co_2Ge, 424 (5.52), 529 (4.42), 553 (4.25), 595 (3.89); Ni_2Ge, 420 (5.70), 426 (5.70), 529 (4.73), 554 (4.63), 595 (4.27); Cu_2Ge, 416 (5.61), 542 (4.28), 594 (3.74); Zn_2Ge, 425 (5.47), 517 (3.61), 556 (4.31), 594 (3.90).

$(H_2)_2$Sn. This compound was prepared by refluxing a dry C_6H_6 solution containing 100 mg (0.12 mmol) of $[(L^1)Sn^{IV}(OH)_2]$ and 180 mg (0.27 mmol) of H_2L^2 under a nitrogen atmosphere for 12 h. The solvent was evaporated, and the resulting residue was loaded onto a neutral alumina column. The desired product was eluted with $CHCl_3$, after which it was recrystallized using a CH_2Cl_2−hexane mixture. Yield: 60%. MS: *m*/*z* $(H_2)_2Sn$ ($C_{142}H_{106}N_{12}O_2Sn$) 2131, $[M]^+$; 1459, $[M - C_{47}H_{35}N_4O]^+$; 788, $[M - 2(C_{47}H_{35}N_4O)]^+$; 673, $[C_{47}H_{36}N_4O]^+$. UV−visible (CH_2Cl_2): λ_{nm} (log ϵ) 420 (5.77), 431 (5.76), 518 (4.64), 559 (4.64), 603 (4.62), 650 (3.60).

$(VO)_2$Sn, $(Co)_2$Sn, $(Ni)_2$Sn, $(Cu)_2$Sn, and $(Zn)_2$Sn. These trimers were prepared in a manner analogous to that described above for the synthesis of $(H_2)_2$Sn, but by replacing H_2L^2 with the corresponding metalloporphyrins. In each case, 50 mg (0.065 mmol) of $[(L^1)Sn^{IV}(OH)_2]$ was refluxed with an excess (0.3−0.4 mmol) of $[(L^2)M]$ (M = $V^{IV}(O)$, Co^{II}, Ni^{II}, Cu^{II}, and Zn^{II}) in dry C_6H_6 under a nitrogen atmosphere for ca. 12−16 h. The solvent was evaporated, and the resulting solids were purified as described above for $(H_2)_2$Sn. Yields ranged typically between 50% and 60%. UV−visible (CH_2Cl_2): λ_{nm} (log ϵ), $(VO)_2$Sn**,** 427 (5.72), 552 (4.32), 602 (4.01); Co_2Sn, 429 (5.61), 530 (4.53), 558 (4.50), 602 (4.12); Ni_2Sn, 417 (5.79), 428 (5.81), 528 (4.81), 561 (4.52), 603 (4.12); Cu_2Sn, 416 (5.32), 427 (5.14), 541 (4.44), 564 (4.12), 603 (3.99); Zn_2Sn, 421 (5.39), 434 (5.28), 552 (4.57), 602 (3.90).

B. Methods. UV−visible spectra were recorded with a Jasco model 7800 UV−visible spectrophotometer. Concentration of the samples used for these measurements ranged from about 2×10^{-6} M (Soret bands) to 5×10^{-5} M (Q-bands). Steady state fluorescence spectra were recorded using a Jasco model FP-777 spectrofluorimeter. The emitted quanta were detected at a right angle to the incident beam. The utilized concentrations of the fluorophores were such that the optical densities (OD) at the excitation wavelengths were always less than 0.2. The fluorescence quantum yields (ϕ_f) were estimated by integrating the areas under the fluorescence curves and by using *meso*-5,10,15,20-tetraphenylporphyrin (H_2L^1) (ϕ_f = 0.11 in CH_2Cl_2) or (*meso*-5,10,15,20-tetraphenylporphyrinato)zinc(II) ($[(L^1)Zn^{II}]$, ϕ = 0.036 in CH_2Cl_2) as standards.[52,53] Refractive index corrections have been incorporated while reporting the fluorescence data in various solvents.[54]

^{1}H NMR (1D and 2D) spectra were recorded with a Bruker NR-200 AT-FT NMR spectrometer using $CDCl_3$ as the solvent and tetramethylsilane (TMS) as an internal standard. The proton-decoupled ^{31}P NMR

(46) Perrin, D. D.; Armarego, W. L. F.; Perrin, D. R. *Purification of Laboratory Chemicals*, 2nd ed.; Pergamon: Oxford, 1980.
(47) Fuhrhop, J.-H.; Smith, K. M. In *Porphyrins and Metalloporphyrins*; Smith, K. M., Ed.; Elsevier: Amsterdam, 1975; p 769.
(48) Barbour, T.; Belcher, W. J.; Brothers, P. J.; Rickard, C. E. F.; Ware, D. C. *Inorg. Chem.* **1992**, *31*, 746.
(49) Kadish, K. M.; Xu, Q. Y. Y.; Maiya, B. G.; Barbe, J.-M.; Guilard, R. *J. Chem. Soc., Dalton Trans.* **1989**, 1531.
(50) Maskasky, J. E.; Kenney, M. E. *J. Am. Chem. Soc.* **1973**, *95*, 1443.
(51) Little, R. G. *J. Heterocycl. Chem.* **1978**, *15*, 203
(52) Quimby, D. J.; Longo, F. R. *J. Am. Chem. Soc.* **1975**, *97*, 5111.
(53) Harriman, A.; Davila, J. *Tetrahedron* **1989**, *45*, 4737.
(54) Lackowwicz, J. R. *Principles of Fluorescence Spectroscopy*; Plenum: New York, 1983.

spectra were also recorded with the same instrument albeit with an operating frequency of 80.5 MHz and with 85% H_3PO_4 as an external standard. ESR spectra were recorded at 100 K with a JEOL JM-FE3X spectrometer with diphenylpicrylhydrazide (DPPH) as an ESR standard. FAB mass spectra were recorded with a JEOL SX 102/DA-6000 mass spectrometer/data system. Cyclic voltammetric experiments (CH_2Cl_2 and 0.1 M tetrabutylammonium perchlorate, TBAP) were performed on a Princeton Applied Research (PAR) 174A polarographic analyzer coupled with a PAR 175 universal programmer and a PAR RE 0074 $x-y$ recorder, as detailed in our previous studies.[43,44,55−59]

Care was taken to avoid the entry of direct, ambient light into the samples in all the spectroscopic and electrochemical experiments. Unless otherwise specified, all the experiments were carried out at 293 ± 3 K.

Results

A. Synthesis. Schemes a and b in Figure 1 illustrate syntheses of the various trimeric arrays investigated during this study. Synthesis of $(H_2)_2P$ (scheme a) had been accomplished earlier[44] by condensing $[(L^1)P^VCl_2]^+$ [43] and H_2L^2 in refluxing pyridine.[60] Analogous trimeric arrays $(H_2)_2Sn$ and $(H_2)_2Ge$ (scheme b) were synthesized during the present study, not by starting with the dichloro complexes but by reacting the corresponding dihydroxo analogues $[(L^1)Sn^{IV}(OH)_2]$ and $[(L^1)Ge^{IV}(OH)_2]$ with an excess of H_2L^2 in refluxing C_6H_6 for 12 h. The desired compound was obtained after column chromatographic purification and recrystallization in each case. A series of trimeric arrays of the type M_2M' (M = (VO), Co, Ni, Cu, or Zn and M′ = P, Ge, or Sn) were obtained by employing two different synthetic strategies. In the first method, 50−60% yields of these hybrid, "transition metal−metalloid" porphyrin arrays were obtained by adopting essentially a method similar to that employed for the synthesis of $(H_2)_2M'$ with the only difference being that $[(L^2)M]$ replaced H_2L^2. The second method involved transition metal insertion into the two axial free-base units of preformed $(H_2)_2P$ and gave 70−95% yields of the desired products. Adaptation of this latter method and using $POCl_3$ as the "metalloid carrier" afforded the "all-phosphorus" trimer P_3.

B. Spectroscopy. Preliminary characterization of these new arrays was carried out by FAB-MS and UV−visible spectroscopic methods. The mass spectrum of $(H_2)_2P$ showed a minor peak at 2059 ascribable to the mass (m/z) of $[(H_2)_2P]^+OH^-$ ($[M + OH]^+$, $C_{142}H_{107}N_{12}O_3P$) and the major molecular ion peak at 2042 ($[M]^+$, $C_{142}H_{106}N_{12}O_2P$). Subsequent peaks appearing at m/z = 1370 and 699 can be ascribed to the detachment of one ($[M - C_{47}H_{36}N_4O]^+$) and two ($[M - 2(C_{47}H_{36}N_4O)]^+$) axial free-base subunits from the basal P^V porphyrin. $(H_2)_2Ge$ and $(H_2)_2Sn$ also showed similar characteristic mass spectral fragmentation patterns but, because they are devoid of any counterion in their structure, the peak ascribable to the $[M + OH]^+$ moiety was absent in the spectra of these arrays. Each array also showed an intense peak at m/z = 673 that is ascribable to the mass of H_2L^2 ($C_{47}H_{36}N_4O$).

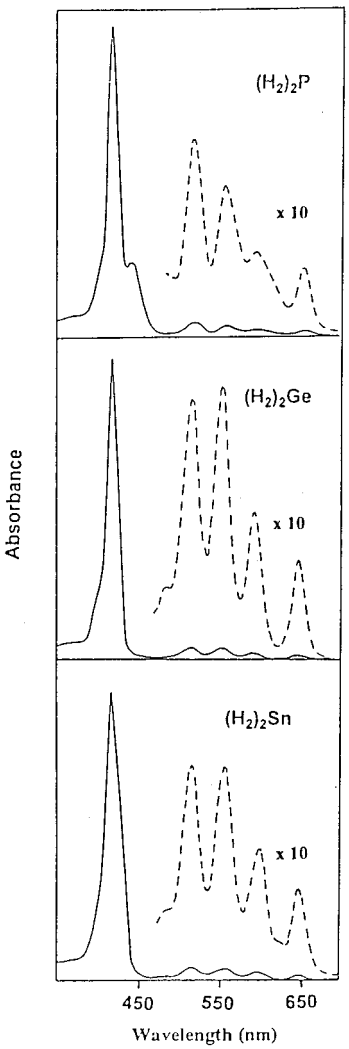

Figure 2. UV−visible spectra of $(H_2)_2P$, $(H_2)_2Ge$, and $(H_2)_2Sn$ in CH_2Cl_2.

The band positions at the maximum absorbance values (λ_{max}) observed in the UV−visible spectrum (CH_2Cl_2) and also the molar extinction coefficient (ϵ) values for each investigated array are summarized in the Experimental Section. Representative spectra of the free-base-containing trimers are illustrated in Figure 2. A comparison of the UV−visible spectrum of a given trimer with the spectra of the corresponding monomeric porphyrins suggested that the λ_{max} values of the trimers are in the same range as those of the reference compounds. In addition, ϵ values of the bands due to the trimers are nearly equal to the sum of the ϵ values of the corresponding bands of the constituent monomers. Minor variations noticed in the spectral features of the trimers with respect to those of the corresponding monomers can be ascribed to the "substituent effects" (i.e., differences in the axial ligands of P^V, Ge^{IV} and Sn^{IV} porphyrins and the meso substituents of free-base porphyrins/metalloporphyrins).

ESR spectra of Cu_2P and $(VO)_2P$ with those of the monomeric reference compounds $[(L^1)Cu^{II}]$ and $[(L^1)V^{IV}(O)]$ are illustrated in Figure 3. The spectra were analyzed using the spin-Hamiltonians reported for the corresponding tetraarylporphyrin derivatives[61−63] to evaluate the relevant ESR parameters. As

(55) Arounaguiri, S.; Dattagupta, A.; Maiya, B. G. *Proc.−Indian Acad. Sci., Chem. Sci.* **1997**, *109*, 155.
(56) Sirish, M.; Kache, R.; Maiya, B. G. *J. Photochem. Photobiol. A: Chem.* **1996**, *93*, 129.
(57) Hariprasad, G.; Dahal, S.; Maiya, B. G. *J. Chem. Soc., Dalton Trans.* **1996**, 3429.
(58) Arounaguiri, S.; Maiya, B. G. *Inorg. Chem.* **1996**, *35*, 4267.
(59) Sirish, M.; Maiya, B. G. *J. Photochem. Photobiol. A: Chem.* **1995**, *88*, 127.
(60) $(H_2)_2P$ represents the trimeric array in which the two free-base porphyrin units have been axially ligated to a basal P^V porphyrin. Nomenclature of the remaining arrays shown in Figure 1 follows accordingly. Note that positive charges on the P^V porphyrin based arrays have been omitted for clarity.

(61) Subramanian, J. In *Porphyrins and Metalloporphyrins*; Smith, K. M., Ed.; Elsevier: Amsterdam, 1975; p 555.
(62) Kievelson, D.; Lee, S. K. *J. Chem. Phys.* **1964**, *41*, 1896.
(63) Assour, J. M. *J. Chem. Phys.* **1965**, *43*, 2477.

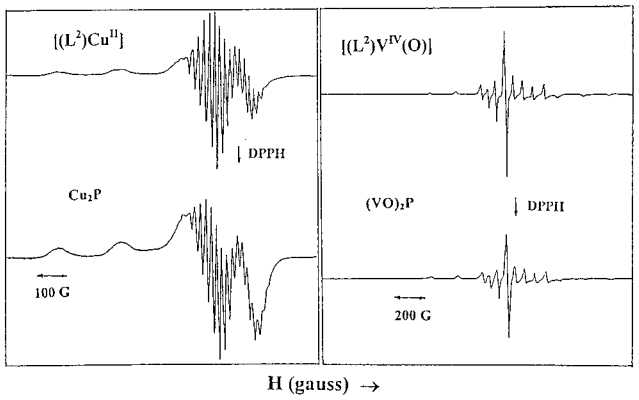

Figure 3. ESR spectra of Cu_2P and $(VO)_2P$ with those of the monomeric reference compounds $[(L^2)Cu^{II}]$ and $[(L^2)V^{IV}(O)]$. In each case, spectra were recorded for $\sim 5 \times 10^{-4}$ M solution of the compound in toluene at 100 ± 3 K. Cu_2P ($[(L^2)Cu^{II}]$): $g_{\|}$, 2.172 (2.185); $g_{\perp}$, 2.040 (2.048); A values ($\times 10^{-4}$ cm^{-1}) $A_{\|}^{M}$, 203 (204); $A_{\perp}^{M}$, 31.6 (30.6); $A_{\|}^{N}$, 16.8 (16.3); $A_{\perp}^{N}$ 15.8 (15.3). $(VO)_2P$ ($[(L^2)V^{IV}(O)]$): $g_{\|}$, 1.960 (1.971); $g_{\perp}$, 1.990 (1.995); A values ($\times 10^{-4}$ cm^{-1}) $A_{\|}^{M}$, 156 (156); $A_{\perp}^{M}$, 56 (55). Error limits: g, ± 0.005; A, $\pm 10\%$.

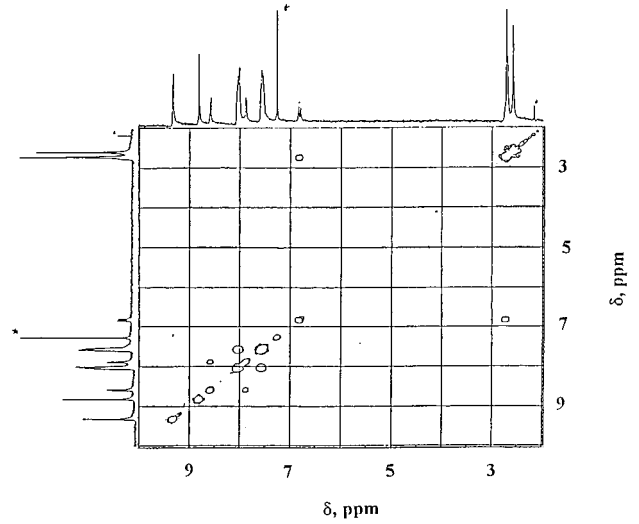

Figure 4. ^{1}H NMR (2D) spectrum of $(H_2)_2P$ in $CDCl_3$. The peak marked with an asterisk (∗) is due to the solvent.

illustrated in Figure 3, the g and A values of Cu_2P and $(VO)_2P$ are similar to the corresponding parameters of $[(L^2)Cu^{II}]$ and $[(L^2)V^{IV}(O)]$. The case is similar with the remaining trimers containing the paramagnetic ions in that the evaluated g and A values are quite close to those of the corresponding monomeric porphyrins. It should be noted here that no $\Delta M_s = \pm 2$ transition at lower magnetic fields has been observed for any of these arrays.

On the other hand, ^{1}H NMR investigations revealed that certain specific spectral features observed for the protons on the axial free-base porphyrins/metalloporphyrins are quite different from those observed for the same protons in the spectrum of H_2L^1 or $[(L^1)M]$. Figure 4 gives the 2D NMR spectrum of $(H_2)_2P$, and a similar spectrum has been observed for the corresponding germanium and tin analogues. ^{1}H NMR data of all of the diamagnetic arrays investigated in this study are summarized in Table 1. Spectra were analyzed on the basis of the resonance position and integrated intensity data as well as the proton-to-proton connectivity information revealed in the COSY spectra to arrive at the structures of these new compounds. Thus, all eight pyrrole-β protons of the phosphorus(V) porphyrin (protons of the type **a**, see Figure 5) in $(H_2)_2P$ resonate

Table 1. ^{1}H NMR[a] and ^{31}P NMR[b] Data

	δ, ppm						
compd	β-pyrrole (central) (a)	β-pyrrole (axial) (b−d)	bridging phenyl (e, f)	−NH (g)	*meso*-tolyl (h, i)	−CH_3 (j, k)	^{31}P
$(H_2)_2P$	9.34 (8H, d) $J = 3.4$	7.89 (4H, d) 8.60 (4H, d) $J = 4.8$ 8.83 (8H, s)	6.86 (4H, d) 2.74 (4H) $J = 7.9$	−2.99 (4H, s)	8.04 (20H, m) 7.56 (20H, m)	2.74 (18H, s) 2.59 (12H, s)	−194
$(H_2)_2Ge$	9.43 (8H, s)	8.21 (4H, d) 8.70 (4H, d) $J = 4.8$ 8.86 (8H, s)	6.72 (4H, d) 2.32 (4H, d) $J = 7.8$	−2.80 (4H, s)	8.45 (8H, d) 8.21 (16H, m) 7.75 (20H, m)	2.89 (18H,s) 2.83 (12H, s)	
$(H_2)_2Sn$	9.38 (8H, d) $J = 6.1$	8.15 (4H, d) 8.60 (4H, d) $J = 4.8$ 8.80 (8H, s)	6.55 (4H, d) 2.45 (4H, d) $J = 8.0$	−2.90 (4H, s)	8.35 (8H, d) 8.05 (12H, m) 7.50 (20H, m)	2.65 (18H, s) 2.60 (12H, s)	
P_3	9.18 (8H, d) $J = 3.9$	8.22 (4H, m) 8.89 (12H, m)	6.60 (4H, d) 2.69 (4H, d) $J = 8.0$		7.89 (8H, d) 7.70 (12H, d) 7.47 (20H, m)	2.54 (18H, s) 2.47 (12H, s)	−196 −229
$(Ni)_2P$	9.28 (8H, d) $J = 3.1$	7.96 (4H, d) 8.49 (4H, d) $J = 4.8$ 8.71 (8H, s)	6.60 (4H, d) 2.65 (4H) $J = 8.0$		7.81 (20H, m) 7.51 (20H, m)	2.65 (18H, s) 2.64 (12h, s)	−194
$(Ni)_2Ge$	9.25 (8H, s)	7.99 (4H, d) 8.51 (4H, d) $J = 4.8$ 8.70 (8H, s)	6.33 (4H, d) 2.65 (4H) $J = 8.2$		8.23 (8H, d) 7.85 (12H, m) 7.48 (20H, m)	2.64 (30H, s)	
$(Ni)_2Sn$	9.33 (8H, s)	8.03 (4H, d) 8.49 (4H, d) $J = 4.6$ 8.71 (8H, s)	6.34 (4H, d) 2.31 (4H, d) $J = 8.0$		8.28 (8H, d) 7.86 (12H, m) 7.46 (20H, m)	2.64 (30H, s)	
$(Zn)_2P$	9.32 (8H, d) $J = 3.5$	7.93 (4H, d) 8.63 (4H, d) $J = 4.7$ 8.87 (8H, s)	6.83 (4H, d) 2.70 (4H) $J = 7.8$		8.02 (20H, m) 7.55 (20H, m)	2.70 (18H, s) 2.59 (12H, s)	−193
$(Zn)_2Ge$	9.28 (8H, s)	8.06 (4H) 8.64 (4H, d) $J = 4.0$ 8.90 (8H, s)	6.52 (4H, d) 2.75 (4H) $J = 7.5$		8.25 (8H, d) 8.06 (12H, m) 7.61 (20H, m)	2.75 (12H, s) 2.71 (18H, s)	
$(Zn)_2Sn$	9.37 (8H, d) $J = 6.3$	8.19 (4H, d) 8.64 (4H, d) $J = 4.8$ 8.92 (8H, s)	6.65 (4H, d) 2.62 (4H, d) $J = 7.4$		8.29 (8H, d) 8.01 (12H, m) 7.55 (20H, m)	2.75 (30H, s)	

[a] Spectra were measured in $CDCl_3$ using TMS as an internal standard; J values are in hertz; Error limits: δ, ± 0.01 ppm. [b] Spectra were measured in $CDCl_3$ using 85% H_3PO_4 as an external standard. Error limits δ, ± 2 ppm.

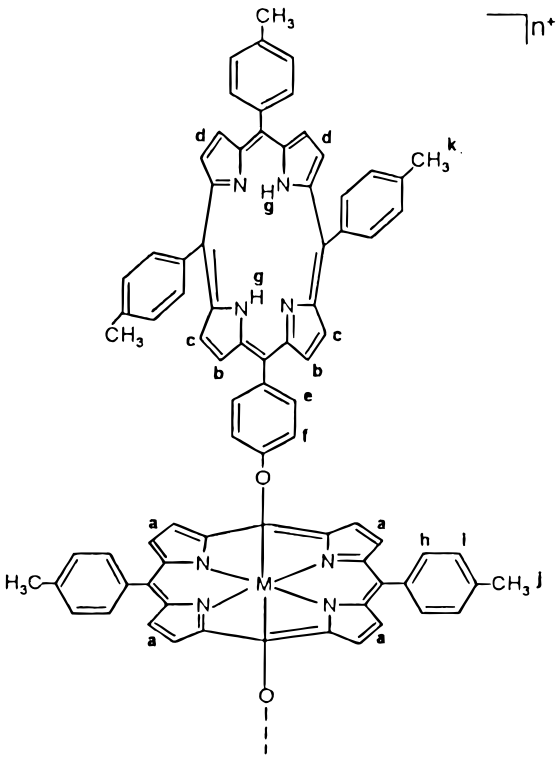

Figure 5. Illustration of the various types of protons present in the investigated arrays (see text and Table 1).

at 9.34 ppm. On the other hand, pyrrole-β proton signals of the axial free-base porphyrins of this trimer are seen to be shifted to the upfield region (compared to those on H_2L^1 or H_2L^2) and also split into a singlet (8.83 ppm (s, 8H)) and a pair of doublets (8.60 ppm (d, 4H) and 7.89 ppm (d, 4H); $^3J_{HH} = 4.8$ Hz). We analyze that four pyrrole-β protons of the type b and four others of the type c (both facing the central porphyrin, see Figure 5), being differently affected by the ring current of the central metalloid porphyrin, resonate as two separate doublets and that the remaining eight pyrrole-β protons on the two free bases (type d) resonate as a singlet[64] under our experimental conditions. This analysis intrinsically assumes a symmetric (but not necessarily parallel) orientation of the two axial free bases with respect to the plane of the central porphyrin ring. The assumption is consistent with the general symmetry observed in the ^{1}H NMR spectrum and, specifically, with the symmetry observed for the resonances due to protons on the axial aryloxy bridges. While protons meta to the "oxo" group (type e) resonate at 6.86 ppm (d, 4H, $J = 7.9$ Hz), those ortho to the "oxo" group (type f) appear at 2.74 ppm (4H) (see the proton connectivity pattern in the 2D NMR spectrum, Figure 4). Interestingly, resonances due to the inner imino protons (type g) of the axial free-base porphyrins are also shielded and appear at -2.99 ppm (s, 4H), as compared to the corresponding protons of H_2L^1 and H_2L^2, both of which resonate at -2.71 ppm**.** The protons on the aryloxy bridges and the imino protons thus simultaneously experience the shielding effect of the central porphyrin and the deshielding effect of the axial porphyrins.[65] Trimeric arrays $(H_2)_2$Sn and $(H_2)_2$Ge and all of the metal−metalloid arrays of the type M_2M' which contain diamagnetic metal ions (M = Zn or Ni and M′ = P, Sn, or Ge) also exhibited similar shielding and splitting patterns in their ^{1}H NMR spectra with the exception that the spectra of M_2M' arrays were devoid of the inner imino proton resonances, Table 1.

^{31}P NMR spectra of the phosphorus-containing arrays have also been measured during this study. The proton-decoupled ^{31}P NMR signal observed for $(H_2)_2$P at -194 ppm is in the typical range for hexacoordinated phosphorus compounds.[66] The ^{31}P resonances of arrays $(M)_2$P, where M = Zn and Ni, also appeared in the same region, but the all-phosphorus array P_3 showed two characteristic resonances, one at -196 ppm (central porphyrin) and the other at -229 ppm (axial porphyrins), see Table 1.

The influence of phosphorus in these arrays has been manifested in the ^{1}H NMR spectra as well. For example, in the ^{1}H NMR spectrum of $(H_2)_2$P, the eight pyrrole-β protons of the phosphorus porphyrin resonate at 9.34 ppm as a doublet due to a four-bond coupling with the phosphorus atom ($^4J_{PH} = 3.4$ Hz). This is not the case with the corresponding Sn^{IV} and Ge^{IV} arrays. In addition, resonances due to all of the pyrrole-β protons on the three P(V) porphyrins of the "all-phosphorus" array P_3 are split due to the four-bond coupling with the phosphorus atoms (basal porphyrin, protons "a" 9.18 ppm (d, 8H, $J = 3.9$ Hz); axial porphyrins, protons "d and c/b" 8.89 ppm (m, 12 H) and protons "b/c" 8.22 ppm (m, 4H)), Table 1.

C. Electrochemistry. With a view to evaluate energies of the charge transfer states (E_{CT}), which, as will be discussed in a later section of this paper, are useful quantities in analyzing the photochemical properties of these arrays, we have carried out electrochemical investigations with arrays containing photoactive axial subunits (viz., free-base or zinc(II) porphyrins). Figure 6 gives the cyclic voltammetric traces obtained for three representative arrays, and Table 2 summarizes the redox potential data along with that of the relevant monomeric analogues. Each array undergoes up to four reduction steps and up to three oxidation steps in CH_2Cl_2, 0.1 M TBAP. Wave analysis suggested that, in general, while the first two oxidation and reduction steps are reversible ($i_{pc}/i_{pa} = 0.9-1.0$) and diffusion-controlled ($i_{pc}/\nu^{1/2}$ = constant in the scan rate (ν) range 50−500 mV/s) one-electron transfer ($\Delta E_P = 60-70$ mV; $\Delta E_P = 65 \pm 3$ mV for ferrocenium/ferrocene couple) reactions, the subsequent steps are, in general, either quasi-reversible ($E_{pa} - E_{pc} = 90-200$ mV and $i_{pc}/i_{pa} = 0.5-0.8$ in the scan rate (ν) range 100−500 mV s^{-1}) or totally irreversible.[67] An accurate assignment of each redox wave of these arrays to electron transfer reaction involving a given constituent porphyrin subunit has been rendered difficult owing to the overlap of the peaks seen in some instances (e.g., voltammogram of $(H_2)_2$Ge, Figure 6). Nonetheless, on the basis of the redox data of the individual monomers, we have attempted to assign the peaks to basal and axial porphyrins separately. Analysis of the data given in Table 2 reveals that the electrochemical redox potentials of the hybrid trimers are in the same range as those of their corresponding monomeric analogues. It also reveals that the basal porphyrin subunits of both $(H_2)_2$P and Zn_2P are easier to reduce than the corresponding Ge^{IV} and Sn^{IV} analogues, but no peak or peaks

(64) In principle, these protons are also expected to appear as a doublet of doublets. However, given their similar magnetic environments, the differences in chemical shift and coupling constant are very small, causing overlap that can look like a singlet at the employed operating frequency of the spectrometer.

(65) Abraham, R. J.; Bedford, G. R.; McNeillie, D.; Wright, B. *Org. Magn. Reson*. **1980**, *14*, 418.
(66) *Multinuclear NMR*; Mason, J., Ed.; Plenum Press: New York, 1987; p 369.
(67) Nicholson, R. S.; Shain, I. *Anal. Chem*. **1964**, *36*, 706.

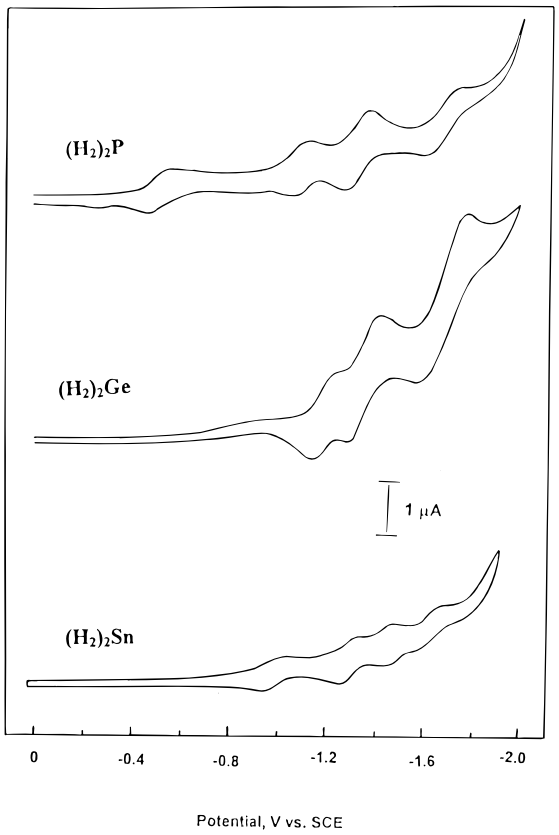

Figure 6. Cyclic voltammograms of $(H_2)_2P$, $(H_2)_2Ge$, and $(H_2)_2Sn$ in CH_2Cl_2, 0.1 M TBAP (scan rate = 100 mV s^{-1}).

Table 2. Redox Potential Data[a]

trimer	potential V, vs SCE reduction	potential V, vs SCE oxidation	E_{CT} ($M^+ M'^-$)	E_{CT} ($M^- M'^+$)
$(H_2)_2P$	−0.46 −0.98 −1.22 −1.60	1.03 1.07	1.49	>3.02
$(H_2)_2Ge$	−1.17 −1.35 −1.60	0.86 1.19[b] 1.33	2.01	2.41
$(H_2)_2Sn$	−1.00 −1.32 −1.49 −1.64	0.93 1.24[b]	1.93	2.71
Zn_2P	−0.45 −1.03 −1.43	0.74 1.01 1.28[b]	1.19	>3.23
Zn_2Ge	−1.12 −1.41[b]	0.76 1.02[b] 1.14 1.35	1.88	2.55
Zn_2Sn	−1.04 −1.48	0.65 0.94 1.33	1.69	2.81

[a] CH_2Cl_2, 0.1 M TBAP; error limits, $E_{1/2}$, ±0.03 V. [b] Quasi-reversible/irreversible.

ascribable to the oxidation of the basal units are noticed in the voltammograms of these P^V arrays. This is probably due to the electron-withdrawing effect exerted by the highly charged, pentavalent phosphorus ion present in the basal porphyrin units of these arrays.[68] Indeed, energies of the possible charge transfer states (i.e., $E_{CT}(M^+M'^-)$ and $E_{CT}(M^-M'^+)$ where M = H_2 or Zn and M′ = P, Sn, or Ge) of these trimers, as evaluated from the redox potential data, testify to this conjecture.

D. Singlet State Activity. Unlike the case with the ground state properties described above, major differences have been noticed between the singlet state activities of the arrays and their corresponding constituent monomers. From the UV−visible data (Figure 2 and Experimental Section) it is clear that, except for $(H_2)_2P$, $(H_2)_2Sn$, and $(H_2)_2Ge$, the axial free-base porphyrins of which are exclusively addressable by excitation at ca. 650 nm, there exists no distinct Q-band that is solely

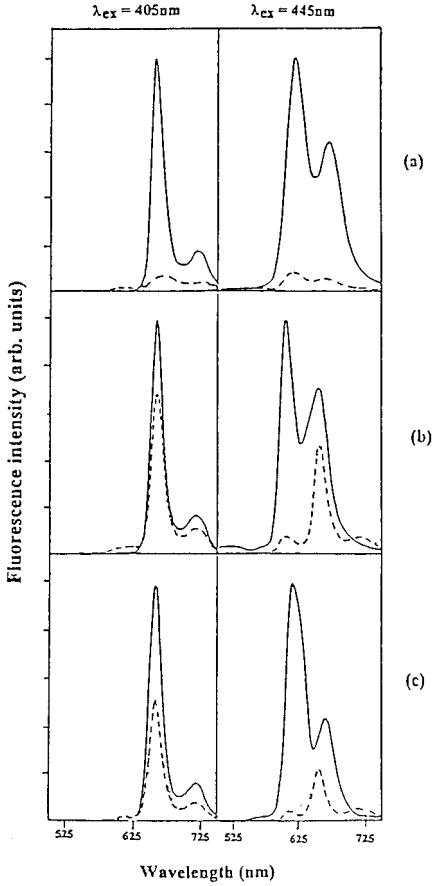

Figure 7. Fluorescence spectra of equiabsorbing solutions (OD at λ_{ex} = 0.14) of the trimers along with those of the corresponding monomers in CH_2Cl_2. λ_{ex} = 405 nm: (a) (—) H_2L^1, (— — —) $(H_2)_2P$; (b) (—) H_2L^1, (— — —) $(H_2)_2Ge$; and (c) (—) H_2L^1, (— — —) $(H_2)_2Sn$. λ_{ex} = 445 nm: (a) (—) $[(L^1)P^V(OH)_2]^+$, (— — —) $(H_2)_2P$; (b) (—) $[(L^1)Ge^{IV}(OH)_2]^+$, (— — —) $(H_2)_2Ge$; and (c) (—) $[(L^1)Sn^{IV}(OH)_2]^+$, (— — —) $(H_2)_2Sn$.

ascribable to the individual monomeric unit of a given array. However, a careful examination of the UV−visible spectra of all of the trimers and their constituent monomers investigated in this study indicated that it is possible to inquire into the individual photochemical activities of the basal and the axial porphyrins by excitation in the Soret band region of the spectra. Thus, we chose to excite the basal P^V, Ge^{IV}, and Sn^{IV} porphyrins at 445 nm (wavelength at which the axial porphyrins show minimum absorption) and the axial free-base and Zn^{II} porphyrins at 405 nm (wavelength at which the basal porphyrins show minimum absorption) during the steady state fluorescence experiments. Representative spectra thus obtained for the three arrays along with the spectra due to the corresponding reference compounds are given in Figure 7. As seen, excitation at either 405 or 445 nm results in quenching of fluorescence for $(H_2)_2P$, $(H_2)_2Sn$, and $(H_2)_2Ge$ in comparison with fluorescence from the corresponding individual, unlinked chromophores. In addition, spectra obtained when, especially, $(H_2)_2Sn$ and $(H_2)_2Ge$ are excited at 445 nm show the fluorescence having originated from the free-base porphyrin (λ_{max} = 650 and 720 nm). The case is similar to the case of arrays endowed with the axial zinc(II) porphyrins, viz., $(Zn)_2P$, $(Zn)_2Sn$, and $(Zn)_2Ge$, in that there is quenching of fluorescence due to both the axial and basal porphyrins.

It should be noted here that while there exists a reduction of fluorescence intensity for each subunit, the spectral shapes and the wavelengths of maximum emission for the individual chromophores of these arrays remain close to those due to the

(68) Liu, Y. H.; Benassy, M.-F.; Chojnacki, S.; D'Souza, F.; Barbour, T.; Blecher, J. W.; Brothers, P. J.; Kadish, K. M. *Inorg. Chem.* **1994**, *33*, 4480.

Table 3. Fluorescence Data[a]

	λ_{em}, nm (ϕ, % Q)[b]							
	toluene		CH_2Cl_2		DMF			
compd	λ_{ex} = 405 nm	λ_{ex} = 445 nm	λ_{ex} = 405 nm	λ_{ex} = 445 nm	λ_{ex} = 405 nm	λ_{ex} = 445 nm	ΔG^1 (eV)[c]	ΔG^2 (eV)[c]
$(H_2)_2P$[d]	657 716 (0.008, 93)	618 669 (0.015, 88)	655 720 (0.003, 97)	620 671 (0.007,94)	657 722 (0.002,98)	621 670 (0.008,93)	−0.45	−0.54
$(H_2)_2Ge$[d]	658 721 (0.034, 69)	605 658 723 (0.003, 95)	657 718 (0.060, 45)	605 658 720 (0.027, 73)	658 722 (0.022, 82)	625 663 724 (0.002, 98)	0.07	−0.06
$(H_2)_2Sn$[d]	658 721 (0.020, 82)	613 658 720 (0.002, 95)	657 719 (0.042, 62)	613 657 719 (0.010, 79)	656 718 (0.010, 92)	657 720 (0.001, 96)	−0.01	−0.11
$(Zn)_2P$	618 664 (0.016, 50)	619 668 (0.026, 78)	620 660 (0.002, 94)	621 670 (0.005, 96)	621 655 (0.002, 94)	622 672 (0.006, 95)	−0.88	−0.84
$(Zn)_2Ge$	603 655 (0.010, 69)	603 655 (0.006, 89)	602 653 (0.006, 83)	602 653 (0.007, 93)	607 660 (0.004, 88)	608 661 (0.004, 96)	−0.19	−0.19
$(Zn)_2Sn$	608 656 (0.003, 91)	603 655 (0.001, 97)	610 662 (0.003, 92)	612 662 (0.001, 98)	614 665 (0.003, 91)	613 657 (0.001, 96)	−0.38	−0.35

[a] Error limits: λ_{em}, ±2 nm; ϕ, ±10%. [b] % Q is defined in eq 1 (see text). [c] ΔG^1 is the free-energy change for the electron transfer from the ground state axial porphyrin to the singlet state central porphyrin. ΔG^2 is the free-energy change for the elctron transfer from the singlet state axial porphyrin to the ground state central porphyrin (see eqs 2 and 3 for details). [d] A small shoulder around 610 ± 10 nm is also noticed for these trimers when excited at 405 nm.

corresponding monomeric entities. Thus, the E_{0-0} (i.e., singlet state energy) values of the individual components of these arrays are assumed to be essentially similar to those of their constituent monomers.[69] Finally, arrays containing the $V^{IV}(O)$, Co^{II}, Ni^{II}, and Cu^{II} porphyrins were found to be either weakly luminescent or totally nonluminescent under our experimental conditions of solvents and excitation wavelengths. Singlet state data of each photoactive array investigated in the present study are summarized in Table 3.

Discussion

A. Design. The architecture of the majority of the previously reported porphyrin arrays can be characterized, in general, by two distinctive structural features: (i) the individual porphyrin subunits have been linked to each other at their peripheral (i.e., β-pyrrole and meso) positions, and (ii) free-base porphyrins and metalloporphyrins have been employed for building the photochemically active, hybrid-porphyrin oligomers. We reasoned that a six-coordinated, bis-axially ligated metalloid−porphyrin can be conveniently employed for the synthesis of "vertically linked", homologous porphyrin arrays and that a proper choice of two different porphyrins should result in the formation of hybrid (unsymmetrical) analogues. Thus, we have recently demonstrated that photochemically active, "vertically linked" porphyrin trimers can be readily constructed by utilizing the axial-bonding capability of P^V porphyrins.[44] The present work has been undertaken to extend the scope of this method and to evaluate the ability of Ge^{IV} and Sn^{IV} porphyrins to act as the basal scaffolds. Here, we provide details of the design, synthesis, spectroscopy, electrochemistry, and singlet state activity of a series of "axial-bonding"-type hybrid porphyrin arrays. In doing so, we have endeavored to compare the characteristic features of the present arrays with those of the porphyrin oligomers previously reported by others and to bring out the scope and limitation of our array-building technology.

Each synthetic step involved during the construction of the arrays investigated in the present study is straightforward and provides good yields of the desired products in pure form. A striking difference in our array-building process in comparison with most of the previously reported processes is that we use "inorganic reactions" (e.g., axial bond formation, metal/metalloid ion insertion) instead of the typical organic reactions employed by other workers. It should be noted here that the use of coordinate−covalent bond formation in the construction of porphyrin oligomers has been well-documented in the literature,[24−42] and, in addition, while this work was in progress, a report describing the synthesis of novel, axial-bonding "wheel-and-axle"-type homologous P^V porphyrin arrays has appeared.[41,42] Nonetheless, we believe that our approach is quite distinct in that it not only provides convenient syntheses of the heterometallic systems but also incorporates the aryloxo spacers (instead of the alkoxo or "metal−nitrogen" spacers employed previously by others[24−42]) between the basal and axial subunits in the architecture of the arrays.[70] Indeed, homologous species such as the "all-phosphorus" array P_3 has been obtained only by the subsequent phosphorus insertion into the hybrid $(H_2)_2P$.[71]

B. Ground State Properties. Analysis of the UV−visible, ESR, and redox potential data suggests the absence of any exciton coupling between the porphyrin rings in these trimers. UV−visible, ESR, and redox features of the covalently linked dimeric and oligomeric porphyrins and also noncovalently bound porphyrin aggregates were investigated earlier in great detail.[72−82] For systems characterized by direct metal−metal (M−M)

(69) E_{0-0} values of H_2, Zn^{II}, P^V, Sn^{IV}, and Ge^{IV} porphyrins are 1.94, 2.07, 2.03, 2.04, and 2.07 (±0.03) eV, respectively.

(70) As rightly pointed out by a referee, lability of the axial bonds can be a concern in this class of compounds and has, indeed, been reported earlier for Sn(IV) porphyrins (e.g.: ref 49). However, the spectral data of the arrays investigated in this study do not suggest any axial bond dissociation occurring under our experimental conditions. The Sn(IV) and Ge(IV) porphyrin based trimers were found to be acid labile.

(71) Even P_3, which contains three phosphorus ions in two different environments (see scheme a in Figure 1), cannot be considered as a true homologous array. Synthesis of the "all-free-base" homologue is clearly outside the scope of this approach.

(72) Eaton, S. S.; Raton, G. R.; Chang, C. K. *J. Am. Chem. Soc.* **1985**, *107*, 3177.
(73) Collman, J. P.; Denisevich, P.; Konai, Y.; Marrocco, M.; Koval, C.; Anson, F. *J. Am. Chem. Soc*. **1980**, *102*, 6027.
(74) Mengersen, C.; Subramanian, J.; Fuhrhop, J.-H. *Mol. Phys*. **1976**, *3*, 893.
(75) Maiti, N. C.; Mazumdar, S.; Periasamy, N. *J. Phys. Chem*. **1998**, *102*, 1528 and references therein.
(76) Collman, J. P.; Wagenknecht, P. S.; Hutchison, J. E. *Angew. Chem., Int. Ed. Engl.* **1994**, *33*, 1537 and references therein.
(77) Ojadi, E.; Selzer, R.; Linschitz, H. *J. Am. Chem. Soc.* **1985**, *107*, 7783.
(78) Thanabal, V.; Krishnan, V. *J. Am. Chem. Soc.* **1982**, *104*, 3644.
(79) Nahor, G. S.; Rabani, J.; Grieser, F. *J. Phys. Chem.* **1981**, *85*, 697.
(80) White, W. I. In *The Porphyrins*; Dolphin, D., Ed.; Academic Press: New York, 1978; Vol. 5, Chapter 7.
(81) Cowan, J. A.; Sanders, J. K. M. *J. Chem. Soc., Perkin Trans.* **1987**, 2395.
(82) Maiya, B. G.; Krishnan, V. *Inorg. Chem*. **1985**, *24*, 3253.

interactions, it has been observed that the *g* and *A* values in the ESR spectra are drastically altered in comparison with the corresponding monomeric reference porphyrins. In addition, depending on the strength of M−M interaction, a $\Delta M_s = \pm 2$ transition at lower magnetic fields has also been reported in a few cases.[72−74,78] Invariance of the *g* and *A* values in comparison with those of $[(L^1)Cu^{II}]$ or $[(L^1)V^{IV}(O)]$ as well as the nonappearance of any $\Delta M_s = \pm 2$ transition in the ESR spectra of our trimers are suggestive of the absence of any M−M interaction between their constituent subunits. Similarly, various types of covalently or noncovalently linked porphyrin dimers (e.g., face-to-face, slipped, etc.) and aggregates (e.g., J, H, and nonspecific) that are characterized by $\pi-\pi$ interaction between the constituent chromophoric units in them have been reported to show distinct UV−visible and electrochemical properties quite different from those of the corresponding monomeric analogues.[75−82] In particular, λ_{max} and ϵ values of the Q-bands and, more importantly, Soret bands as well as the oxidation and reduction potentials of these dimers/aggregates have been reported to be sensitive to the strength of interaction between the monomeric π-planes and geometry of the ensembles. In contrast, UV−visible and electrochemical properties of the trimeric systems reported here are quite similar to those of the monomeric porphyrins forming them. Thus, ESR, UV−visible, and redox data collectively point out that there exists minimum interaction between the individual porphyrins in these arrays. Nonetheless, these data do not provide clues as to the structures of the arrays.

On the other hand, several diagnostic features observed in the NMR spectra of the arrays have been helpful in elucidating their gross structures. Specifically, resonance positions and splitting patterns observed for the pyrrole-β protons of the two axial porphyrins and protons of the two aryloxo bridges are characteristic of these arrays. These protons simultaneously experience the shielding effect of the central porphyrin and the deshielding effect of the axial porphyrins, suggesting that the orientation between the π-planes is of the "vertical" type and certainly not face-to-face. It is expected that an additive shielding effect, as reported for the axial protons of the "wheel-and-axle"-type porphyrins, should be noticed for any porphyrin ensemble having the "face-to-face" juxtaposition of the interacting monomeric subunits.[41,42,76] Thus, it seems likely that a symmetrically disposed vertical (but not necessarily parallel) orientation of the axial subunits is appropriate for our trimers. This interpretation is consistent not only with the results of ESR, UV−visible, and redox data discussed above but also with the similar interpretations made earlier for the "vertically" linked porphyrin arrays and boxes assembled via coordinate−covalent interactions.[24−42]

^{31}P NMR spectral data are illustrative of the local environment around the phosphorus ion in phosphorus-containing arrays. The ^{31}P resonances for these arrays occur in a region that is typical of hexacoordinated phosphorus and, moreover, are sensitive to the nature of the axial ligands. Ligation by chloro or "oxo" groups at the axial positions could be readily identified on the basis of the ^{31}P NMR data.

C. Excited State Properties. The fact that electronic structures of the excited states of the individual subunits in these trimers are similar to those of the corresponding monomers is indicated by the observation that shapes of the fluorescence bands and E_{0-0} values of these arrays are not different from those of the unlinked monomeric porphyrins. However, fluorescence due to both the basal and axial porphyrins is considerably quenched in comparison with that due to the monomeric chromophores. The quenching efficiency values (*Q*) have been evaluated using the quantum yield data, eq 1, where, ϕ(trimer)

$$Q = (\phi(\text{ref}) - \phi(\text{trimer}))/\phi(\text{ref}) \quad (1)$$

and ϕ(ref) refer to the quantum yields of a given array and the appropriate reference compound, respectively. While H_2L^1 ($[(L^1)Zn^{II}]$) has been chosen as the common reference compound for studies with excitation into the 405 nm bands of $(H_2)_2P$ (Zn_2P), $(H_2)_2Sn$ (Zn_2Sn), and $(H_2)_2Ge$ (Zn_2Ge), monomers $[(L^1)P^V(OH)_2]^+$, $[(L^1)Sn^{IV}(OH)_2]$, and $[(L^1)Ge^{IV}(OH)_2]$ are conceived to be the appropriate reference compounds for studies carried out with excitation into the 445 nm bands of these trimers. The % *Q* values thus calculated range between 45 and 98 (Table 3), indicating the participation of additional pathway(s) for the singlet state decays of the individual subunits of these arrays.

Various radiative and nonradiative intramolecular processes can be conceived to participate in the excited state decay of these novel, hybrid-type, donor−acceptor (D−A, in fact, D_2-A or $D-A_2$) systems.[83] Among these, an electronic energy transfer (EET) from the central main group element containing porphyrin (M′) to the axial free-base/zinc(II) porphyrin (H_2/Zn) and also the photoinduced electron transfer (PET) from H_2/Zn (ground state) to the singlet state of the central porphyrin (^{1}M′) and also that from $^1H_2/^1$Zn to M′ seem to be more probable as revealed by the thermodynamic considerations based on the redox potential (E_{CT}) and singlet state energy (E_{0-0}) data, Figure 8. These considerations have further revealed that the presence of different metal/metalloid ions inside the constituent porphyrin subunits of these arrays serves to readily modulate the efficiencies of the EET and PET reactions.

As illustrated in Figure 7 and data given in Table 3, excitation at either 405 (λ_{ex} at which H_2/Zn absorbs predominantly) or 445 nm (λ_{ex} at which M′ absorbs predominantly) results in quenching of fluorescence for $(H_2/Zn)_2P$, $(H_2/Zn)_2Sn$, and $(H_2/Zn)_2Ge$ in comparison with fluorescence from the corresponding individual, unlinked chromophores. In addition, spectra obtained when, especially, $(H_2)_2Sn$ and $(H_2)_2Ge$ were excited at 445 nm show fluorescence having originated from the free-base porphyrin (λ_{em}(max) = 650 and 720 nm), indicating an intramolecular EET in these arrays. The energy transfer efficiency (% EET) follows the order $(H_2)_2P$ (<5%) ≪ $(H_2)_2Sn$ (68% ± 10%) < $(H_2)_2Ge$ (83% ± 10%) as evaluated from an overlap of the excitation spectra with the corresponding absorption spectra.[84] In a similar set of experiments conducted with arrays having zinc(II) porphyrins as the axial ligands, it was not possible to evaluate the % EET because of overlap of the bands due to the donor and acceptor chromophores.[84] On the other hand, efficiency of the PET from the ground state axial porphyrins (M = H_2/Zn) to the singlet manifold of the central porphyrin (^{1}M = ^{1}P, ^{1}Sn, or ^{1}Ge) that is possible in these arrays can vary as $(H_2/Zn)_2Ge$ < $(H_2/Zn)_2Sn$ ≪ $(H_2/Zn)_2P$, a trend which is

(83) A variety of excited state processes including enhanced internal conversion and intersystem crossing, ion association (for cationic P^V porphyrins), excitation energy transfer (EET), photoinduced electron transfer (PET), etc. can be thought of as being operative in the quenching of fluorescence observed for these arrays. Indeed, EET has been demonstrated to be operative in the fluorescence quenching observed for the triads that are similar in their architecture to H_2P and its derivatives (see ref 40). Currently, there exists no direct or indirect evidence to show the correspondence between the trends observed for the ϕ values and the extent of ion association, internal conversion, and intersystem crossing in these systems.

(84) The % EET values have been obtained from an overlap of the corrected and normalized excitation (λ_{em}(max) = 720 nm where only H_2 emits) spectra with the corresponding absorption spectra as described in our previous studies.[56,59] Such an exclusive λ_{em}(max) where only the axial Zn^{II} porphyrins emit is clearly lacking in Zn_2Ge, Zn_2Sn, and Zn_2P.

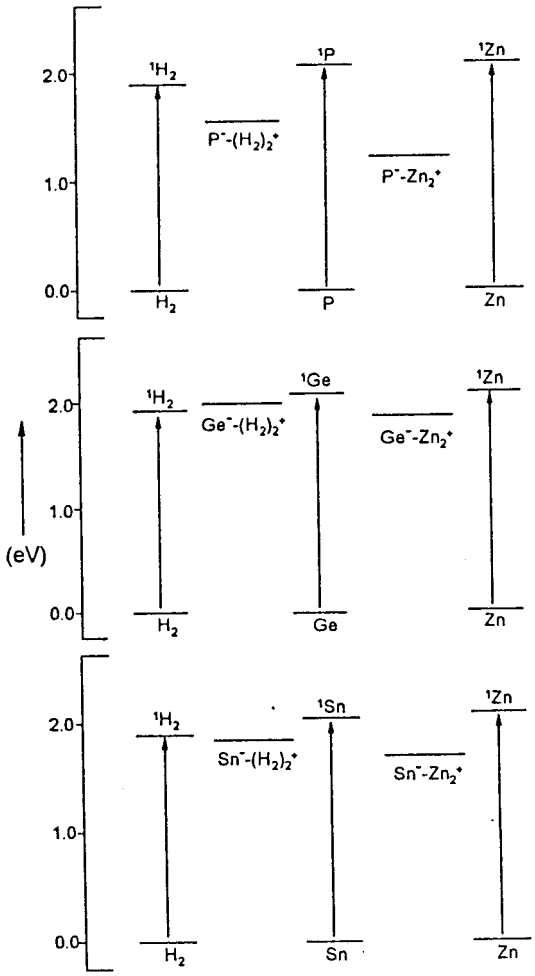

Figure 8. Energies of the singlet and charge transfer states pertaining to the photoactive arrays investigated in this study.

consistent with the free-energy change for this electron transfer process, $\Delta G(M \rightarrow {}^1M')$ (eq 2).[85] The values of $\Delta G(M \rightarrow {}^1M')$,

$$\Delta G(M \rightarrow {}^1M') = E_{CT}(M^+M'^-) - E_{0-0}(M') \qquad (2)$$

as estimated using the $E_{CT}(M^+M'^-)$ (Table 2)[85] and E_{0-0} (M′) data,[69] range between 0.07 and −0.88 eV, Table 3. Thus, the low ϕ values observed upon excitation of these systems at 445 nm can be rationalized in terms of the competing energy transfer and electron transfer reactions with the electron transfer pathway being predominant in the P^V porphyrin arrays (see Figure 8).

In contrast, fluorescence quenching observed upon excitation of these systems at 405 nm seems primarily due to a PET from $^1H_2/^1Zn$ to the linked M′ as neither is the energy transfer from the axial free-base or zinc(II) porphyrins to the central porphyrin thermodynamically feasible nor was it experimentally detected in this study. The PET from $^1H_2/^1Zn$ to the linked M′ has been found to be exoergic for each investigated array. The free-energy change for this PET, $\Delta G(^1M \rightarrow M')$,[85] has been estimated using eq 3.

$$\Delta G(^1M \rightarrow M') = (E_{CT}(M^+M'^-) - E_{0-0}(M) \qquad (3)$$

The general dependence of ϕ values on $\Delta G(^1M \rightarrow M')$ and somewhat on the solvent polarity (see Table 3) suggests that this might indeed be the case. Overall, the singlet state decays of the $(H_2/Zn)_2M'$ arrays can be represented as follows.[86]

$$(M_2)M' \xrightarrow{405\ nm} {}^1(M_2)M' \xrightarrow{EET} (M_2)^1M' \qquad (4)$$

$$(M_2)M' \xrightarrow{405\ nm} {}^1(M_2)M' \xrightarrow{PET} (M_2)^{+\bullet}(M')^{-\bullet} \qquad (5)$$

$$(M_2)M' \xrightarrow{445\ nm} {}^1(M_2)M' \xrightarrow{PET} (M_2)^{+\bullet}(M')^{-\bullet} \qquad (6)$$

M = H2 or Zn and M′ = P, Ge, or Sn

Finally, the hybrid M_2M' trimers with M other than zinc were all found to be nonfluorescent, probably due to the presence of paramagnetic or heavy metal ions in these systems.

Conclusions

In conclusion, a series of P^V, Ge^{IV}, and Sn^{IV} porphyrin-based, "axial-bonding"-type hybrid trimers have been readily constructed by employing a new "building-block" approach. The approach is modular in nature, and it involves simple "inorganic" reactions such as axial bond formation of main group element containing porphyrins and insertion of metal/metalloid ions into porphyrin cavities. A facile and predetermined modulation of the redox and photophysical properties of these soluble arrays can be achieved simply by substituting the porphyrin cavities with various metal/metalloid ions either during or after the array-building process. It should be possible to extend this "building-block" approach and construct higher, branched-chain oligomers. It should also be possible to synthesize trimers having one metalloid porphyrin and at least two different metalloporphyrins ("truly" hybrid trimers) in their architecture. Currently, our efforts are directed toward the construction of such giant-sized, multi-metal/metalloid-containing porphyrin arrays.

Acknowledgment. Financial support received for this work from CSIR (New Delhi) is gratefully acknowledged. L.G. thanks the UGC for a research fellowship.

Supporting Information Available: Tables containing the complete set of data on the UV−visible, ESR, redox, and fluorescence characteristics. This material is available free of charge via the Internet at http://pubs.acs.org.

IC990326C

(85) Note that $E_{CT}(M^+M'^-)$ is susceptible to changes in the solvent polarity parameters and can influence both $\Delta G(M \rightarrow {}^1M')$ and $\Delta G(^1M \rightarrow M')$ values.

(86) An enhanced intersystem crossing and/or a weak EET (singlet state energies of Zn^{II} and group 14 or group 15 element containing porphyrins are close to each other) cannot be entirely ruled out. Further studies inquiring into the detailed photophysical properties of these trimers by the application of time-resolved techniques are in progress.